Biosensors and Bioelectronics 88 (2017) 196–203

Contents lists available at ScienceDirect

Biosensors and Bioelectronics

journal homepage: www.elsevier.com/locate/bios

Improved DET communication between cellobiose dehydrogenase and a gold electrode modified with a rigid self-assembled monolayer and green metal nanoparticles: The role of an ordered nanostructuration

P. Bollella[a], F. Mazzei[a], G. Favero[a], G. Fusco[a], R. Ludwig[c], L. Gorton[b], R. Antiochia[a,*]

[a] Department of Chemistry and Drug Technologies, Sapienza University of Rome, P.le Aldo Moro 5, 00185 Rome, Italy
[b] Department of Analytical Chemistry/Biochemistry and Structural Biology, Lund University, P.O.Box 124, SE-221 00 Lund, Sweden
[c] Food Biotechnology Laboratory, Department of Food Science and Technology, BOKU – University of Natural Resources and Life Sciences, Muthgasse 18, A-1190 Vienna, Austria

ARTICLE INFO

Keywords:
Cellobiose dehydrogenase
Direct electron transfer
Gold nanoparticles
Silver nanoparticles
Biphenyl-4,4′-dithiol
Lactose

ABSTRACT

Efficient direct electron transfer (DET) between cellobiose dehydrogenase from *Corynascus thermophilus* (*Ct*CDH) and a novel gold electrode platform, obtained by covalent linking of green AuNPs and AgNPs modified with a dithiol self-assembled monolayer, consisting of biphenyl-4,4′-dithiol (BPDT), was presented. The green AuNPs and AgNPs were synthesized using quercetin as reducing agent at room temperature. TEM experiments showed that the AuNPs and AgNPs were circular in shape with an average diameter of 5 and 8 nm, respectively. Cyclic voltammetry of *Ct*CDH immobilized onto the AuNPs/BPDT/AuE and the AgNPs/BPDT/AuE electrode platforms were carried out and compared with naked AuE, BPDT/AuE, AuNPs/AuE, and AgNPs/AuE. A pair of well-defined redox waves in neutral pH solution due to efficient DET of CtCDH was present with both MNPs/BPDT/AuE platforms. No DET communication was found with platforms without MNPs linked to BPDT. The apparent heterogeneous electron transfer rate constants (k_S) of *Ct*CDH were calculated to be $21.5 \pm 0.8\ s^{-1}$ and $10.3 \pm 0.7\ s^{-1}$, for the AuNPs/BPDT/AuE and the AgNPs/BPDT/AuE platforms, respectively.

The modified electrodes were successively used to develop an eco-friendly biosensor for lactose detection. The *Ct*CDH/AuNPs/BPDT/AuE based biosensor showed the best analytical performances with an excellent stability, a detection limit of 3 μM, a linear range between 5 and 400 μM and a sensitivity of $27.5 \pm 2.5\ \mu A\ cm^{-2}\ mM^{-1}$. Such performances were favorably compared with other lactose biosensors reported in literature.

The biosensor was successively tested to quantify lactose content in real milk and cream samples. No significant interference present in the sample matrices was observed.

1. Introduction

Studies of direct electron transfer (DET) between redox enzymes and electrodes represent an area of extensive research for developing bioelectronic devices such as biosensors and biofuel cells. However, it is well known in the literature that most redox enzymes are not able to reveal DET, because the active site of the enzyme is usually deeply buried within the protein structure (Ghindilis et al., 1997). Nanomaterial based electrodes are able to promote efficient DET reactions because of their large surface area for protein loading as well as their excellent biocompatibility (Pumera et al., 2007; Jianrong et al., 2004; Bollella et al., 2016).

Several approaches of electrode nanostructuration have been developed in order to increase the electroactive area of the electrode (Minteer et al., 2012; Wang et al., 2012; Mazzei et al., 2015; Taurino et al., 2016), including single- and multi-walled carbon nanotubes (Liu et al., 2005; Favero et al., 2015), graphene (Pumera, 2011; Carbone et al., 2015) and metal nanoparticles (Wang et al., 2004; Pingarron et al., 2008).

Among all kind of nanomaterials, metal nanoparticles (MNPs) play an important role in making electrode modifications, because of their high surface area-to-volume ratios and high surface energy, which facilitate the immobilization of several kinds of proteins, allowing to act as electron conducting pathways between the prosthetic groups of the enzymes and the electrode surface (Yañez-Sedeño et al., 2005; Ludwig et al., 2010; Loo et al., 2012; Katz and Willner, 2004; Chen et al., 2012). Another advantage of the use of MNPs is the improved stability of enzyme based electrodes. This can be due to a reduced enzyme

* Corresponding author.
E-mail address: riccarda.antiochia@uniroma1.it (R. Antiochia).

http://dx.doi.org/10.1016/j.bios.2016.08.027
Received 13 June 2016; Received in revised form 9 August 2016; Accepted 10 August 2016
Available online 24 August 2016
0956-5663/

leaching from the electrode because of the strong adsorption of proteins onto the uncoated nanometer-sized colloidal MNPs allowing the protein to retain its biological activity (Baudhuin et al., 1989).

Green synthesis of MNPs has recently become a cheep alternative way for a sustainable and safe production of MNPs (Shah et al., 2015; Cinelli et al., 2015). Several approaches have been reported in the literature, which employ extracts from a variety of different plant species in combination with a variety of acids and metal salts (Ghoreishi et al., 2011; Elia et al., 2014; Makarov et al., 2014). The principal biomolecules present in plant extracts utilized as reducing agents to form MNPs are proteins, polyphenols, vitamins and sugars, such as L-ascorbic acid, gallic acid and quercetin (Wang et al., 2007; Nune et al., 2009; Iravani, 2011). However, most synthesis methods utilizing these biomolecules require high temperatures such as the synthesis using starch and glucose as reducing agents at high temperature for 20 h (Raveendran et al., 2003) or the synthesis using L-ascorbic acid at 80 °C (Mat Zain et al., 2014; Xiong et al., 2011) or the need of microwave assistance (Valodkar et al., 2011; Singh et al., 2016). Moreover these methods are influenced by several variables which are difficult to control and can affect the method reproducibility (Nadagouda and Varma, 2008; Philip, 2010; Zargar et al., 2011).

MNPs can be deposited onto an electrode surface by different approaches: drop-casting (Krueger et al., 2011), covalent linkage (Yang et al., 2006) or electrodeposition directly from the metal precursor (Saha et al., 2012). One of the easiest ways to perform electrode modification is the covalent linkage by using the self-assembled monolayer (SAM) technique (Chaki and Vijayamohanan, 2002; Arya et al., 2009). In recent years, MNPs were self-assembled into two-dimensional or three-dimensional superstructures by using several cross-linkers such as dithiols, diamines, thiolsiloxanes etc. (Wink et al., 1997; Wang et al., 2004). It has been recently demonstrated that aromatic dithiols work better than alkanedithiols because of their enhanced conductivity and low suppleness. In particular it has been found that biphenyl 4,4′-dithiol (BPDT), compared with alkanethiol molecules, is more conductive and forms a monolayer with a vertical molecular configuration, probably because of the rigid structure of the phenyl rings and the π stacking of the molecule (Liang et al., 2007; Matei et al., 2012).

Cellobiose dehydrogenase (CDH) is receiving great attention in recent years in the development of biosensors and biofuel cells (Ludwig et al., 2010; Ludwig et al., 2013) because of its ability to show DET (Lindgren et al., 2001; Schulz et al., 2016; Matsumura et al., 2012; Tasca et al., 2011) for a large number of substrates including sugars, such as glucose and lactose (Tasca et al., 2013; Harreither et al., 2007). CDH is an extracellular flavocytochrome secreted by wood degrading fungi (Zamocky et al., 2006). It consists of a catalytically active flavin adenine dinucleotide (FAD) containing dehydrogenase domain (DH_{CDH}) connected via a flexible linker region to an electron mediating, heme *b* containing cytochrome domain (CYT_{CDH}). The oxidation of the natural substrate cellobiose fully reduces FAD and the electrons are successively transferred by an internal electron transfer mechanism (IET) to the CYT_{CDH} domain resulting in reduced heme *b* (Schulz et al., 2014). CYT_{CDH} acts as a built-in mediator, which shuttles the electrons to suitable electrodes (Schulz et al., 2016). CHDs are expressed by fungi from the dikariotic phyla Basidiomycota (class I CDHs) and Ascomycota (class II CDHs) with different protein sequences (Ludwig et al., 2013; Zamocky et al., 2008). All CDHs accept cellodextrines, cellobiose and lactose as substrates, some class II CHDs also show activity for glucose (Harreither et al., 2011). CDH obtained from the ascomycete *Corynascus thermophilus* (*Ct*CDH) belongs to class II CDHs (Zafar et al., 2012). Unlike CDHs from basidiomycetes and most class II CDHs that show more efficient DET at acidic pHs, CtCDH catalyzes the oxidation of the mono- and disaccharides at neutral pHs, thus allowing DET at physiological conditions.

The aim of this work was to improve the DET efficiency between *Ct*CDH and a novel gold electrode platform, obtained by covalent linking of green AuNPs and AgNPs with a dithiol self-assembled monolayer, biphenyl-4,4′-dithiol (BPDT). The AuNPs and AgNPs were synthesized using quercetin as reducing agent in aqueous solution at room temperature. The novelty of this approach is the use of green MNPs together with BPDT, which allowed an ordered linkage of MNPs because of the low suppleness of its molecule. The so modified electrode was used to develop an eco-friendly biosensor for lactose detection. To the best of our knowledge this is the very first time that BPDT has been used with MNPs for the development of a lactose biosensor. The modified electrode platforms, *Ct*CDH/AuNPs/BPDT/AuE and *Ct*CDH/AgNPs/BPDT/AuE, shown in Scheme 1, were compared with naked gold electrode, BPDT/AuE and MNPs/AuE in absence and in presence of lactose. The study aimed at investigating the effects of the different electrode modifications on DET between *Ct*CDH and the electrode surface. The electrochemical characterization and optimization of the lactose biosensor obtained with the *Ct*CDH/AuNPs/BPDT/AuE platform is also presented in this work. Finally the applicability of the developed biosensor was tested for lactose detection in real milk and cream samples.

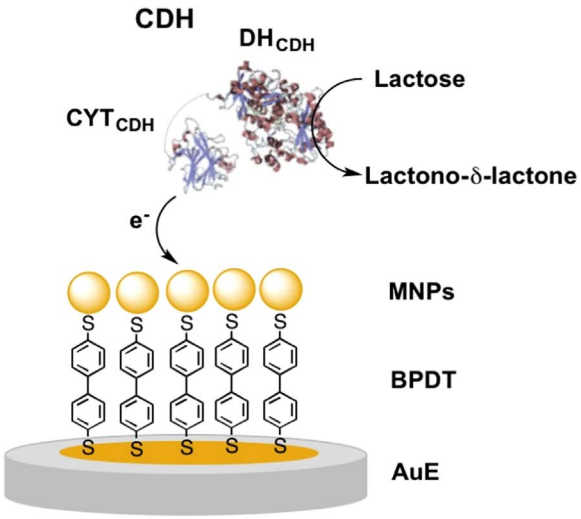

Scheme 1. *Ct*CDH/MNPs/BPDT/AuE platform and DET between *Ct*CDH and the modified electrode.

2. Experimental

2.1. Chemicals and reagents

3-(N-morpholino)propanesulfonic acid (MOPS), β-lactose, sulfuric acid (H_2SO_4), hydrogen peroxide (H_2O_2), D-glucose, D-cellobiose, biphenyl-4,4′-dithiol (BPDT), chloroauric acid ($HAuCl_4{\cdot}3H_2O$), quercetin (QUC), silver nitrate ($AgNO_3$), sodium phosphate monobasic (NaH_2PO_4), sodium phosphate dibasic (Na_2HPO_4) and potassium chloride (KCl) were obtained from Sigma Aldrich (St. Louis, MO, USA), calcium chloride ($CaCl_2$) was purchased from Merck KgaA (Darmstadt, Germany), dialysis membranes (Spectrapor, MWCO 12–14 kDa) were purchased from Spectrum Medical Industires (CA, USA). *Ct*CDH (E.C. 1.1.99.18) (volumetric activity with cytochrome *c* at pH 7.5=53 U ml^{-1}, protein concentration=8.4 mg ml^{-1}) was used for electrode modification. *Ct*CDH was purified from the culture supernatant of the ascomycete *Corynascus thermophilus* (CBS 405.69) obtained from the Centralbureau voor Schimmelcultures (Baarn, The Netherlands). Cultivation and purification of the enzyme were similar to previously reported protocols for *Myriococcum thermophilum* CDH (Zamocky et al., 2008). The enzyme was stored in a 50 mM acetate buffer (pH 5.5 at −80 °C).

Real samples (2% lowfat milk, light cream, whipped cream and 80% lactose-reduced milk) were bought in a local supermarket and carefully

diluted in 50 mM MOPS buffer at pH 7.4 in a ratio 1:250, before analysis. All solutions were prepared using Milli-Q water (18.2 MΩ cm, Millipore, Bedford, MA, USA).

2.2. Synthesis of green AuNPs and AgNPs

The synthesis of AuNPs and AgNPs was carried out using quercetin (QUC) to reduce $HAuCl_4$ and $AgNO_3$, respectively. $HAuCl_4$ and $AgNO_3$ were solubilized in 50 mM PBS buffer at pH 7; quercetin was solubilized in a 1 M NaOH solution with a final concentration of 1 mM, then diluted in 50 PBS buffer at pH 7, and adjusting the pH of the final solution to pH 7.0. The synthesis was performed by mixing a 50 μM solution of QUC with a 300 μM solution of $HAuCl_4$ or $AgNO_3$, in a total reaction batch volume of 10 ml, at room temperature in 50 PBS buffer at pH 7. In both cases the mixture changed color from orange to deep purple for AuNPs and to yellow for AgNPs within a few seconds, because of the formation of the MNPs colloidal solutions. A complete characterization of the synthetized NPs was carried out and reported completely in our previous paper (Bollella et al., submitted).

2.3. TEM experiments

Transmission electron microscopy (TEM) was undertaken with a Philips/FEI BioTwin CM120 TEM microscopy (Hillsboro, OR, USA). Two drops of the synthesized colloidal samples were deposited on a polymer thin copper grid followed by solvent evaporation under vacuum.

2.4. Electrode preparation and modification

Polycrystalline gold electrodes (diameter=1.6 mm, BASi, West Lafayette, IN, USA) were cleaned by incubation in Piranha solution for 2 min (1:3 mixture of conc·H_2O_2 with H_2SO_4, *CAUTION: Piranha solution is especially dangerous, corrosive and may explode if contained in a closed vessel, it should be handled with special care*), then with polishing cloths with deagglomerated alumina slurry of 1 μm diameter (Struers, Ballerup, Denmark), successively sonicated in ultrapure water for 5 min and finally electrochemically cleaned in 0.5 M H_2SO_4 by cycling 20 times between −0.3 and 1.7 V vs. $Ag|AgCl_{sat\ KCl}$ at a scan rate of 300 mV/s.

The electrode modification was carried out by immersing the electrodes in a 10 mM ethanolic solution of biphenyl-4,4′-dithiol (BPDT) overnight at room temperature. The electrodes were successively gently rinsed with ultrapure water and dried under a stream of N_2. MNPs colloidal solutions were drop-cast onto the top of gold electrodes and left to dry at room temperature for 20 min, then gently rinsed with water to avoid any excess of MNPs unreacted with the SAM. Finally, 3 μL of the *Ct*CDH solution were drop-cast onto the so modified surface, left to dry, and then entrapped by covering it with a pre-soaked dialysis membrane, which was fixed with a plastic holder (Haladjian et al., 1994).

AuNPs/AuE and AgNPs/AuE electrodes were obtained following the same procedure described above without the step of BPDT immobilization. Figure SM1 (Supplementary material) shows the SEM images of AuNPs/AuE and AgNPs/AuE electrodes before and after washing, thus confirming that the MNPs remain onto the electrode surface after the washing procedure.

2.5. Electrochemical measurements and electrochemical apparatus

Cyclic voltammetry experiments were carried out using a PalmSens potentiostat (model Emstat^2, Palm Instruments BV, Utrecht, The Netherlands) equipped with PSTrace, version 4.5. A conventional three-electrode electrochemical cell was used for all experiments performed with an Ag|AgCl (sat. KCl) as reference electrode, a platinum wire as counter electrode and a modified gold electrode as working electrode.

Flow injection experiments were performed with a three electrode potentiostat (Zäta Elektronik, Höör, Sweden). The enzyme-modified gold electrode, inserted into a wall-jet flow-through amperometric cell and positioned at a constant distance (1–2 mm) from the inlet nozzle (Appelqvist et al., 1985), was used as working electrode, an $Ag|AgCl_{0.1\ KCl}$ electrode as reference electrode and a platinum wire as counter electrode. The electrochemical cell was connected to a flow injection system consisting of a peristaltic pump (Gilson, Villier-le-Bel, France) and a six-port valve electrical injector (Rheodyne, Cotati, CA, USA). A 50-ll aliquot of the substrate was applied by a loop mounted onto the injector. The resulting electrical current was recorded on a strip chart recorder (Kipp & Zonen, Utrecht, The Netherlands). All measurements were performed at room temperature.

3. Results and discussion

3.1. Green synthesis and characterization of AuNPs and AgNPs

Both AuNPs and AgNPs were synthesized at room temperature using QUC as reducing agent and $HAuCl_4$ and $AgNO_3$ as metal precursors, respectively, according to the reactions shown in Figure SM2 (see Supplementary material). The solution turned from orange to purple and yellow color, indicating the formation of AuNPs and AgNPs, respectively. The most important reaction parameters, reaction time and metal precursor concentration, have been optimized with UV–Vis spectrophotometry, as already described in a previous paper (Bollella et al., submitted). The reaction time was very short (20 min for AgNPs and 30 min for AuNPs) and the synthesis showed a high reaction yield and great reproducibility. MNPs were characterized by transmission electron microscopy (TEM), in order to study their shape, dimensions and size distributions and the results are shown in Fig. 1. Both AuNPs and AgNPs show an almost homogeneous size distribution, spherical form and crystalline structure without aggregates and clusters. The real diameter of the AuNPs and AgNPs resulted in 5.5 ± 0.6 and 8.4 ± 0.3 nm, respectively. A more detailed characterization of the MNPs (EDS spectroscopy, dynamic light scattering, zeta potential) is reported in our previous work (Bollella et al., submitted).

3.2. Electrochemistry of CtCDH on modified MNPs/BPDT/Au electrodes

In order to demonstrate the influence of an ordered nanostructuration on the efficiency of DET communication between *Ct*CDH and the electrode surface, CVs experiments were initially carried out with CDH immobilized onto a bare Au electrode. As shown in Fig. 2a (black curve), no redox waves relative to DET communication between the CYT_{CDH} domain and the electrode surface are visible. The AuE surface was then modified by self-assembling biphenyl-4,4′-dithiol, in order to allow a proper orientation of the enzyme onto the electrode surface. However, once again, no clear redox waves were obtained, as shown in Fig. 2b (black curve). The modification with a bifunctional reagent generally largely enhances the analytical response as the SAM molecule links the enzyme facilitating a DET reaction with the electrode surface (Ludwig et al., 2010). This unexpected result can be ascribed to the fact that BPDT has a terminal -SH group instead of the terminal alcohol or acid groups of most SAMs, which can covalently link only a very small amount of enzyme; moreover at the working pH (7.4) the -SH groups of BPDT are negatively charged (pK_a=6.6) and create an electrostatic repulsion with CtCDH, which is in its anionic form (pI=3.8), thus not favoring the electron transfer from CtCDH to the electrode surface.

Fig. 2(c and d, black curves) shows the CVs of the *Ct*CDH/AuNPs/AuE (C) and *Ct*CDH/AgNPs/AuE (D). With the modification of the electrode with MNPs without SAM a pair of redox waves start to become visible, indicating DET communication of *Ct*CDH, favored by the MNPs. The efficiency of DET is increased with the nanostructura-

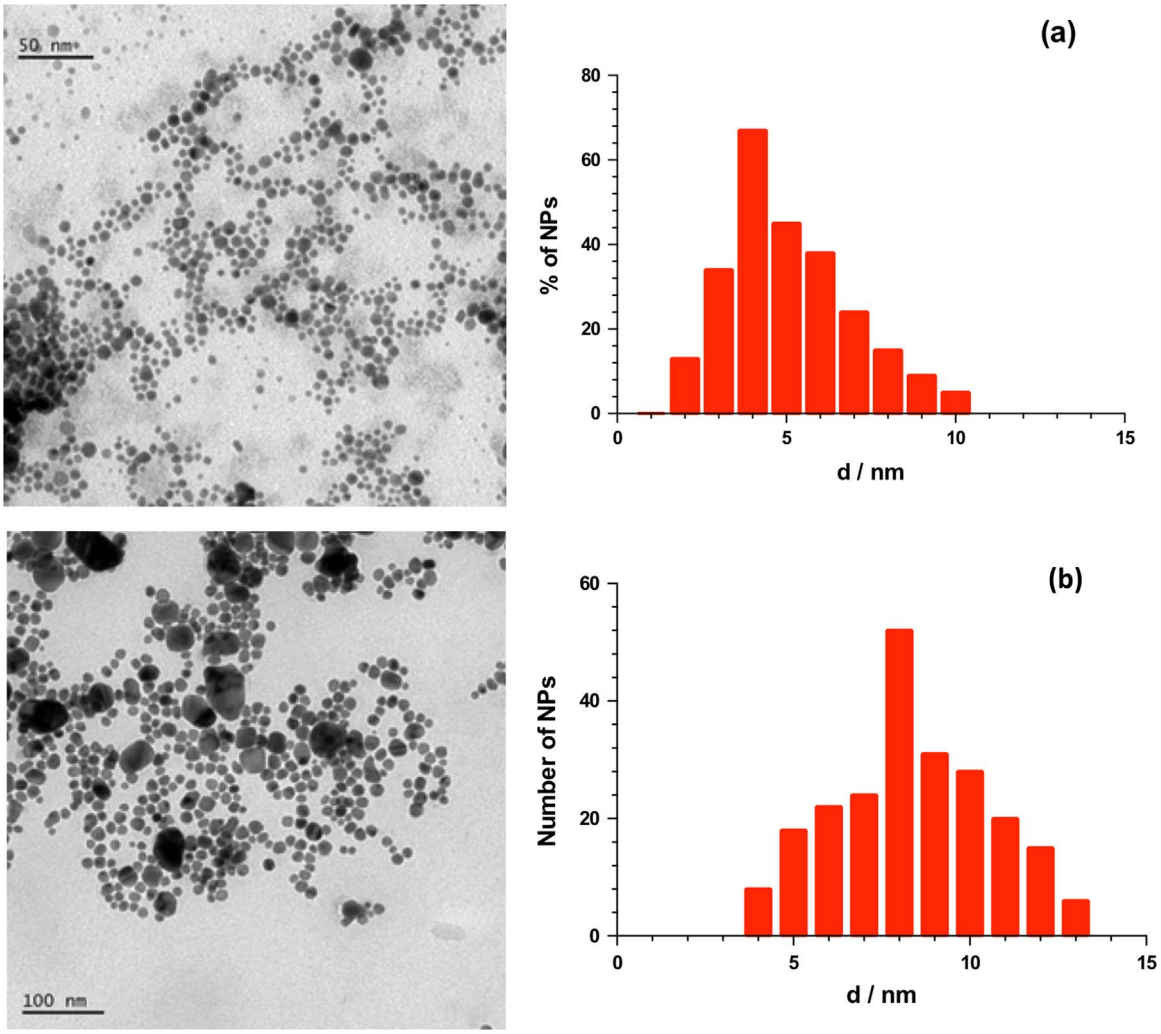

Fig. 1. (a) TEM image of a colloidal solution of AuNPs formed by reduction of Au^{3+} ions using quercetin (left) and size distribution (right); (b) TEM image of a colloidal solution of AgNPs formed by reduction of Ag^{+} ions using quercetin (left) and size distribution (right).

tion of the electrode surface, because there is a higher probability that the enzyme is immobilized in the correct orientation for DET.

Successively, AgNPs and AuNPs were drop-cast onto the BPDT modified electrode. Fig. 2(e and f, black curves) shows CVs relative to CtCDH/BPDT/Au electrodes modified with AgNPs (Fig. 2e) and AuNPs (Fig. 2f). As expected, a pair of well-defined high redox waves, originating from the oxidation and reduction of the heme *b* cofactor located in the CYT_{CDH}, are visible in both cases. DET is now favored by a combined effect of a higher fraction of immobilized *Ct*CDH molecules in DET orientation and a larger number of CtCDH molecules immobilized, due to the presence of the MNPs linked to the SAM, which allow an ordered nanostructuration of the electrode surface. The formal potential (E°′) of the heme *b* group of CYT_{CDH}, evaluated as the midpoint of the oxidation and reduction peak potentials, resulted to be approximately −96 mV and −114 mV vs. $Ag|AgCl_{sat\ KCl}$ for AuNPs and AgNPs, respectively, close to literature values for *Ct*CDH immobilized onto gold electrodes (Harreither et al., 2012a, 2012b). The peak separation between the anodic and cathodic peak potentials were 44 mV and 50 mV at ν=1 mV s^{-1} for AuNPs and AgNPs, respectively, in good agreement with the typical values of a surface confined redox process (Haladjian et al., 1994; Laviron, 1979).

It should be noted that with AuNPs modified electrodes the redox peak currents are almost ten times higher than those with AgNPs modified electrodes. This result may be ascribed to the fact that the AuNPs are smaller and slightly more positively charged than the AgNPs at pH 7.4 (zeta potential values −28.5 ± 1.4 mV and −39.0 ± 1.3 mV for the AuNPs and the AgNPs, respectively) (Bollella et al., submitted). A less electrostatic repulsive environment for the CYT_{CDH} (pI 3.8) is created with AuNPs, thus enhancing DET and allowing a larger enzyme loading onto the electrode surface without influencing the electrochemical behavior of the enzyme.

The electroactive area (A_{EA}) and the roughness factor of the electrode surface of the different platforms were studied. Both parameters exhibited to be largely enhanced with the MNPs/BPDT/AuE platforms, thanks to the ordered nanostructuration Table SM1, (see Supplementary material). Even though the geometrical surface areas are identical, the electrode modified with MNPs linked to BPDT shows a higher real surface area for CDH immobilization compared to naked Au electrodes and to the electrodes modified with the cross-linker agent BPDT or MNPs, separately (Ward et al., 2013).

The scan rate effect was investigated on the DET reaction of the immobilized CtCDH at the MNPs/BPDT/Au electrodes. The CVs at the AuNPs/BPDT/AuE and AgNPs/BPDT/AuE are presented in Fig. SM3a and b (see Supplementary material). It is possible to see that the anodic and cathodic peak currents were linearly proportional versus the scan rate in the range 5–300 mV s^{-1} (Fig. SM3c), indicating a surface controlled electrochemical process.

Further analysis of the CVs allowed calculating the apparent heterogeneous electron transfer rate constants (k_s) for the redox reaction between CtCDH and AuNPs/BPDT/AuE and AgNPs/BPDT/AuE electrodes using the Laviron's method (Laviron, 1979). From the slopes of the linear part of the trumpet plot reported in Fig. SM4d the

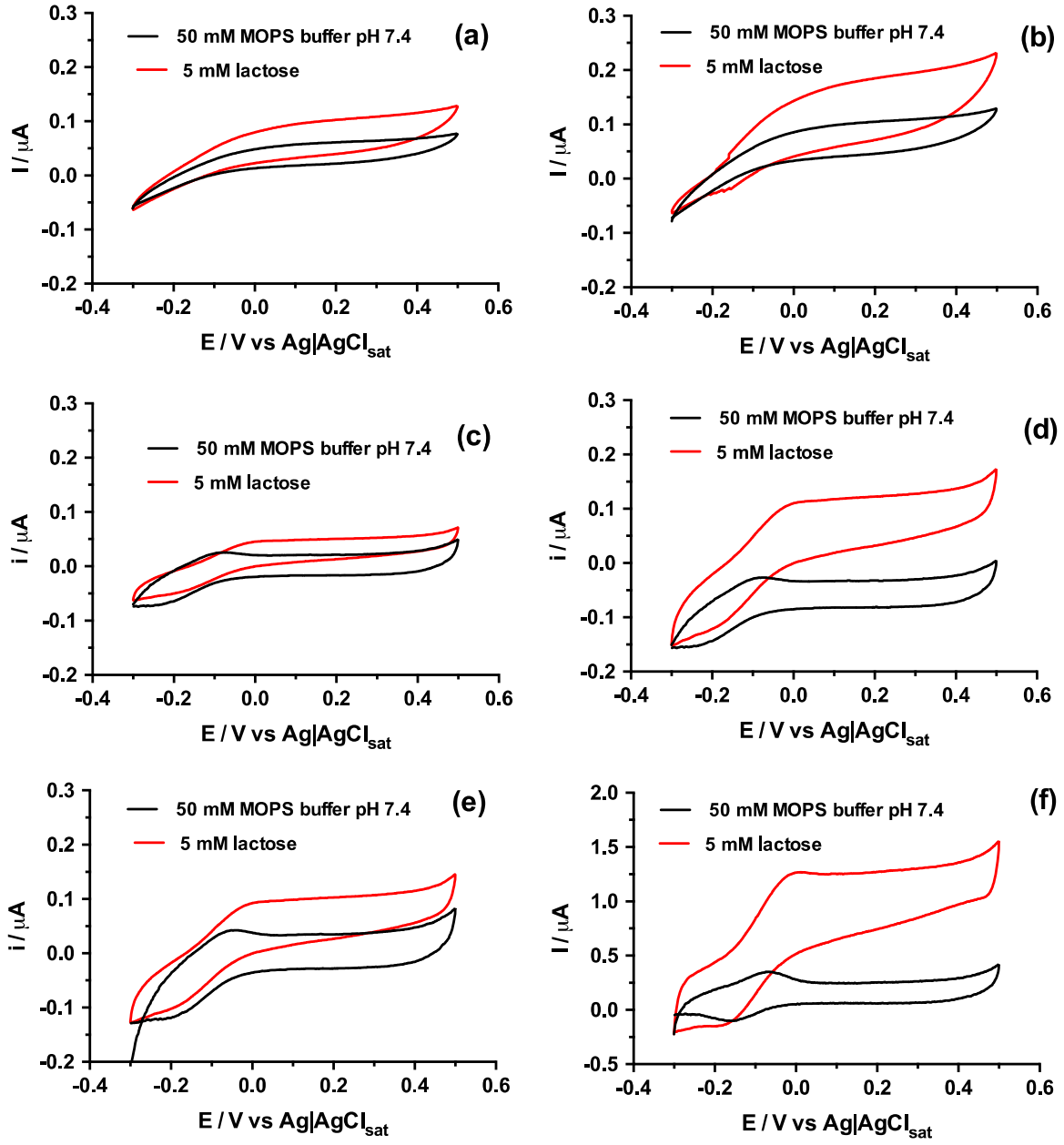

Fig. 2. CVs of *Ct*CDH immobilized onto AuE (a), DPDB/AuE (b) AgNPs/AuE (c), AuNPs/AuE (d), AgNPs/DBDP/AuE (e), AuNPs/DBDP/AuE (f) in absence (black curves) and in presence (red curves) of 5 mM lactose in 50 mM MOPS buffer pH 7.4. Scan rate 1 mV/s. (For interpretation of the references to color in this figure legend, the reader is referred to the web version of this article.).

values can be determined to be 0.49 and 0.47 for the AuNPs and the AgNPs modified electrodes, respectively. Thereafter, the k_s values were calculated according to Laviron's derivation of the Butler-Volmer theory (Eq. (1)) (Laviron, 1979) for a two-electron reaction of a surface confined electroactive species and resulted in 21.5 ± 0.8 s^{-1} and 10.3 ± 0.7 s^{-1} for the AuNPs and the AgNPs modified electrodes, respectively (ν between 5 and 300 mV s^{-1}):

$$\log k_s = \alpha \log(1-\alpha) + (1-\alpha)\log(RT/nF\nu) - \alpha(1-\alpha)nF\Delta E_p/2.3RT \quad (1)$$

where α is the electron transfer coefficient, n is the number of electron, ΔE_p is the separation of the redox peak potentials, ν the scan rate and F, T and R have their usual meanings (F=96.493 C mol^{-1}; T=298 K; R=8.31 J mol^{-1} K^{-1}).

3.3. Electrocatalytic behavior of CtCDH on modified Au electrodes

The electrocatalytic behavior of *Ct*CDH modified electrodes was studied by performing CV experiments in the presence of lactose (Fig. 2, red curves) with the different electrode platforms: AuE (Fig. 2a), BPDT/AuE (Fig. 2b), AgNPs/AuE (Fig. 2c), AuNPs/AuE (Fig. 2d), AgNPs/BPDT/AuE, (Fig. 2e) and AuNPs/BPDT/AuE (Fig. 2f). The CVs clearly show the effects of different electrode modifications towards the electrocatalytic current recorded in the presence of substrate and perfectly agree with the results obtained for DET of CtCDH in the absence of substrate.

With the bare AuE no significant electrocatalytic current is observed, probably because the *Ct*CDH molecules are not properly orientation for DET (Fig. 2a, red curve). With the BPDT/AuE platform a small electrocatalytic current is noted after the addition of substrate (Fig. 2b, red curve) as expected when a cross-linking agent is used, although the current is very low, possibly because of the strong

repulsion between the enzyme and the self-assembled monolayer, both negatively charged at pH 7.4 (Gadogbe et al., 2015). With the modification of the electrode with MNPs the electrocatalytic current for lactose can be observed with a maximum at around 0 V vs. Ag|AgCl, due to the effect of the nanostructuration of the electrode surface (Fig. 2c and d, red curves). AuNPs modified electrodes showed a definitely higher electrocatalytic current probably because at pH 7.4 the AgNPs are less negatively charged than the AgNPs and therefore create a less electrostatic repulsive effect for CtCDH. With the BPDT/MNPs modified electrodes the catalytic currents were higher than with the other electrode platforms (Fig. 2e and f), in accordance with the observations reported in the previous paragraph. These excellent performances can be ascribed to the synergistic effect of nanostructuration and cross-linking, which create a highly packed and ordered nanostructured surface responsible for the enhanced electron transfer. AgNPs and AuNPs are linked through strong covalent bonds with the -SH groups of the SAM, which favor the electron transfer to the electrode thanks to its two aromatic rings. The rigid structure of the molecule, which does not allow any bending onto the electrode surface is another factor that might promote the fast electron transfer from the enzyme. It is easily noted that the AuNPs modified electrode exhibited an electrocatalytic current more than 10 times higher (Fig. 2f, red curve) than that obtained with AgNPs modified electrodes, always probably because the AuNPs are smaller and less negatively charged than the AgNPs.

The results showed that the best electrode platform was shown to be the *Ct*CDH/AuNPs/DBDP/AuE and therefore this platform was used for further experiments.

3.4. Lactose biosensor development

In order to investigate the electroanalytical and kinetic parameters of the *Ct*CDH/AuNPs/BPDT/AuE and *Ct*CDH/AgNPs/BPDT/AuE platforms, the amperometric response to lactose was studied with flow injection analysis (FIA) by successively injecting lactose solutions into the neutral MOPS buffer solution. The fastest peak response was obtained with the AuNPs/BPDT/AuE (3 s), compared to the AgNPs/BPDT/AuE (5 s), probably due to the better electrochemical communication between CtCDH and the electrode surface. Calibration curves for the *Ct*CDH/AuNPs/BPDT/AuE and the *Ct*CDH/AgNPs/BPDT/AuE platforms showed linear response ranges from 5 to 400 μM and from 10 to 400 μM for AuNPs/BPDT/AuE and AgNPs/BPDT/AuE, respectively (R^2=0.99 for both). At higher concentrations the response is no longer linear, thus indicating enzyme saturation (Fig. 3a). The inset in Fig. 3a shows the strict linear response of the biosensor versus lactose concentration. The detection limit was found to be 3 μM for AuNPs/BPDT/AuE and 7.5 μM for AgNPs/BPDT/AuE (S/N=3). The sensitivity for lactose was 27.5 μA mM^{-1} cm^{-2} with the AuNPs/BPDT/AuE platform, almost three times higher than that obtained with the AgNPs modified electrode (10 μA mM^{-1} cm^{-2}).

The characteristics of the lactose biosensor are presented in Table 1. The apparent kinetic parameters (I_{max}, K_M^{app}), obtained by fitting the calibration curves, show a sensible reduction of the apparent Michaelis-Menten constant (K_M^{app}) obtained with AuNPs (844.2 μM) compared to AgNPs ordered nanostructuration (2553.3 μM), suggesting an enhanced enzymatic affinity for the substrate when AuNPs are used. This result can also be explained taking into account that the modification of the electrode with AuNPs creates a more favorable environment for CtCDH compared to AgNPs, allowing the enzyme to correctly orientate its redox centers for an efficient DET.

To date, only a few lactose biosensors have been reported in the literature based on various CDHs (Table SM2) (see Supplementary material) while most other lactose biosensors are based on a cascade of two or three different enzymes (Stoica et al., 2006). In Table SM2 are reported the main analytical characteristics of lactose biosensors based on different types of CDHs. It is interesting to note that the proposed AuNPs/BPDST/AuE biosensor shows a clear extension of the linear range, an enhanced sensitivity and a lower response time compared to other lactose biosensors reported in the literature.

3.5. Stability measurements, interferences evaluation and real samples analysis

The stability and lifetime of the *Ct*CDH/AuNPs/BPDST/AuE biosensor was studied by FIA by measuring the decrease in the electrocatalytic currents after successive injections of lactose. It is possible to observe in Fig. 3b a decrease in the response signal of only 24.3% during continuous injections for 20 days. This result can be due to the ordered nanostructuration of the electrode surface achieved with the concomitant use of BPDT and AuNPs and also to the very small AuNPs dimensions, which can prevent the leaching/detaching of the immobilized enzyme from the electrode surface thus allowing a long term stability of the biosensor.

In order to evaluate the performance of the proposed biosensor for the detection of lactose in real samples, the selectivity of the biosensor was studied by comparing the signal obtained adding equal quantities of interfering compounds (Ca^{2+}, D-cellobiose and D-glucose) and lactose (Harreither et al., 2007). The results are reported in Fig. 3c. It can be observed that the amperometric signal of Ca^{2+} is less than 20% of the response of lactose, while D-cellobiose about 75% and glucose about 15%. As cellobiose and glucose are not present in milk samples, the proposed biosensor can be utilized for lactose detection in real samples with no significant interference. Table 2 shows the results obtained on four different real samples (2% lowfat milk, light cream, whipping cream and 80% lactose-reduced milk). The biosensor *Ct*CDH/AuNPs/BPDT/AuE biosensor allowed the detection of lactose in all samples analyzed with a satisfactory recovery in the range 90–98% (RSD values lower than 4.7%).

4. Conclusions

This work demonstrates the feasible achievement of an efficient DET of a CDH thanks to the ordered electrode nanostructuration realized with a gold electrode modified with a self-assembled monolayer and MNPs. This is the very first time, to the best of our knowledge, that BPDT has been used with AuNPs and AgNPs for the development of a lactose biosensor. The best performances were obtained with the *Ct*CDH/AuNPs/BPDT/AuE platform because AuNPs are smaller and less negatively charged than AgNPs, thus allowing a better orientation and wiring of the enzyme onto the electrode surface. The proposed lactose biosensor can be prepared by a simple and eco-friendly procedure as the MNPs were synthesized according to a green reaction pathway using quercetin as reducing agent which allowed a synthesis at room temperature with a short reaction time, without harmful and expensive reagents, and with high reproducibility. The lactose biosensor was fast-responding and showed a very good stability, excellent sensitivity and a broad linear range. Milk and dairy product matrices did not affect the performance of the biosensor. It can be operated at neutral pH and, unlike lactose biosensors based on class I CDHs, it can also detect glucose. For this reason, the proposed biosensor holds great promises for possible applications as a biofuel cell bioanode suitable to work at human blood conditions.

Acknowledgments

The authors thank the following agencies for financial support: The Swedish Research Council (Vetenskapsradet project 2014-5908), the European Commission (project “Bioenergy” FP7-PEOPLE-2013-ITN-607793).

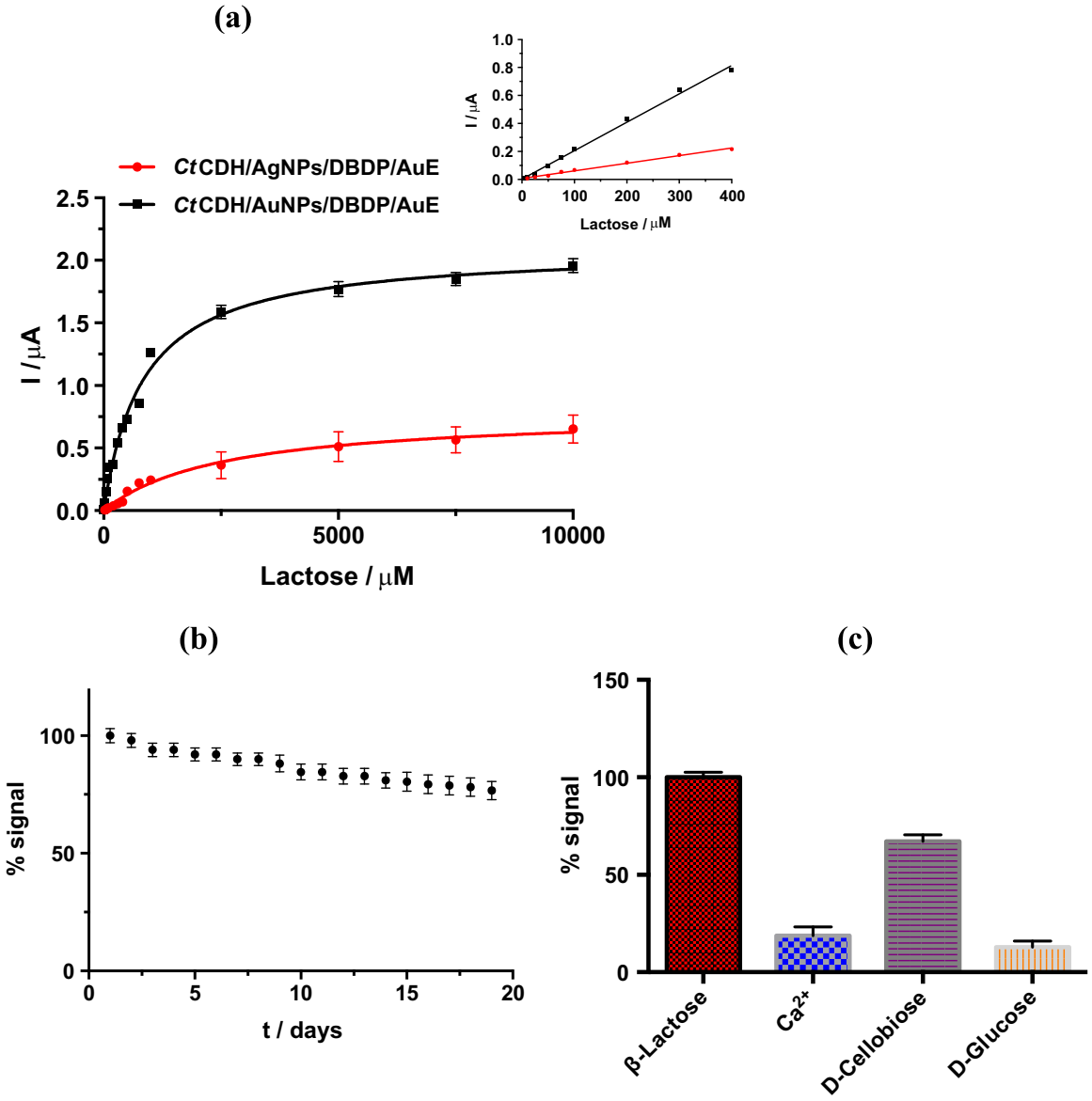

Fig. 3. Calibration graphs for lactose **(a)**; in the inset, the biosensor response in the low-micromolar range; lifetime of *Ct*CDH/AuNPs/DBDP/AuE biosensor in the presence of 200 μM lactose solution in 50 mM MOPS buffer pH 7.4 **(b)**; influence of interfering compounds on lactose response: 1 mM lactose solution (red), 1 mM Ca^{2+} solution (blue), 1 mM D-cellobiose (purple) and 1 mM D-glucose (pink) **(c)**. Buffer: 50 mM MOPS, pH 7.4; applied potential: +0.250 V vs. Ag|$AgCl_{sat}$. (For interpretation of the references to color in this figure legend, the reader is referred to the web version of this article.).

Table 1
Electroanalytical and kinetic parameters of *Ct*CDH biosensors employing different electrochemical platforms obtained by FIA amperometry in 50 mM MOPS buffer, pH 7.4. Applied potential: +0.250 V vs. Ag|$AgCl_{sat}$.

	AuNPs/BPDT/AuE	AgNPs/BPDT/AuE
E_{app}/(V vs Ag|$AgCl_{sat}$)	0.250	0.250
K_M^{app}/(μM)	844 ± 30	2553 ± 39
I_{max}/(μA)	2.1 ± 0.05	0.8 ± 0.04
LOD/(μM)	3	7.5
Linearity range/(μM)	5–400	10–400
Sensitivity/(μA mM^{-1} cm^{-2})	27.5 ± 2.5	10 ± 1
R^2	0.990	0.991

Table 2
Measurements of lactose in real samples diluted 1:250. Experimental conditions: 50 mM MOPS buffer pH 7.4; applied potential: +0.250 V vs. Ag|$AgCl_{sat}$.

Samples	Found value (μM)	Nominal value (μM)	Recovery (%)
2% Lowfat milk	368.6 ± 14.5	384.3 ± 29.2	95.91
Light Cream	440.7 ± 36.9	478.8 ± 53.1	92.04
Whipping Cream	535.3 ± 34.8	594.2 ± 21.6	90.08
80% Lactose-reduced Milk	114.9 ± 12.5	117.3 ± 15.7	97.95

Appendix A. Supplementary material

Supplementary data associated with this article can be found in the online version at doi:10.1016/j.bios.2016.08.027.

References

Appelqvist, R., Marko-Varga, G., Gorton, L., Torstensson, A., Johansson, G., 1985. Anal. Chim. Acta 169, 237–247.
Arya, S.K., Solanki, P.R., Datta, M., Malhotra, B.D., 2009. Biosens. Bioelectron. 24, 2810–2817.
Baudhuin, P., Van der Smissen, P., Beauvois, S., Courtoy, P.J., 1989. Molecular interactions between colloidal gold, proteins, and living cells. In: Hayat, M.A. (Ed.), Colloidal Gold: Principles, Methods, and Applications 2. Academic Press, San Diego,

2–34.
Bollella, P., Fusco, G., Tortolini, C., Sanzò, G., Favero, G., Gorton, L., Antiochia, R., 2016. Biosens. Bioelectron.. http://dx.doi.org/10.1016/j.bios.2016.03.068.
Bollella, P., Schulz, C., Favero, G., Mazzei, F., Ludwig, R., Gorton, L., Antiochia, R., Electroanalysis, accepted for publication
Carbone, M., Gorton, L., Antiochia, R., 2015. Electroanalysis 27, 16–31.
Chaki, N.K., Vijayamohanan, K., 2002. Biosens. Bioelectron. 17, 1–12.
Chen, J.I., Zheng, X.L., Miao, F.J., Zhang, J.N., Cui, X.Q., Zheng, W.T., 2012. J. Appl. Electrochem. 42, 875–881.
Cinelli, M., Coles, S.R., Nadagouda, M.N., Btaszczyński, J., Słowiński, R., Varma, R.S., Kirman, K., 2015. Green Chem. 17, 2825–2839.
Elia, P., Zach, R., Hazan, S., Kolusheva, S., Porat, Z., Zeiri, Y., 2014. Int. J. Nanomed. 9, 4007–4021.
Favero, G., Fusco, G., Mazzei, F., Tasca, F., Antiochia, R., 2015. Nanomaterials 5, 1995–2006.
Gadogbe, M., Chen, M., Zhao, X., Saebo, S., Beard, D.J., Zhang, D., 2015. J. Phys. Chem. C 119, 6626–6633.
Ghindilis, A.L., Atanasov, P., Wilkins, E., 1997. Electroanalysis 9, 661–674.
Ghoreishi, S., Behpour, M., Khayatkashani, M., 2011. Physica E 44, 97–104.
Haladjian, J., Bianco, P., Nunzi, F., Bruschi, M., 1994. Anal. Chim. Acta 289, 15–20.
Harreither, W., Coman, V., Ludwig, R., Haltrich, D., Gorton, L., 2007. Electroanalysis 19, 172–180.
Harreither, W., Sygmund, C., Augustin, M., Narciso, M., Rabinovich, M.L., Gorton, L., Haltrich, D., Ludwig, R., 2011. Appl. Environ. Microbiol. 77, 1804–1815.
Harreither, W., Felice, A.K.G., Paukner, R., Gorton, L., Ludwig, R., Sygmund, C., 2012a. Biotechnol. J. 7, 1359–1366.
Harreither, W., Nicholls, P., Sygmund, C., Gorton, L., Ludwig, R., 2012b. Langmuir 28, 6714–6723.
Iravani, S., 2011. Green Chem. 13, 2638–2650.
Jianrong, C., Yuqing, M., Nongyue, H., Xiaohua, W., Sijiao, L., 2004. Biotechnol. Adv. 22, 505–518.
Katz, E., Willner, I., 2004. Angew. Chem. Int. Ed. 43, 6042–6108.
Krueger, M., Berg, S., Stone, D., Strelcov, E., Dikin, D.A., Kim, J., Cote, L.J., Huang, U., Kolmakov, A., 2011. ACS Nano 5, 10047–10054.
Laviron, E., 1979. J. Electroanal. Chem. 101, 19–28.
Liang, J., Rosa, L.G., Scoles, G., 2007. J. Phys. Chem. C 111, 17275–17284.
Lindgren, A., Gorton, L., Ruzgas, T., Baminger, U., Haltrich, D., Schülein, M., 2001. J. Electroanal. Chem. 496, 76–81.
Liu, Y., Wang, M., Zhao, F., Xu, Z., Dong, S., 2005. Biosens. Bioelectron. 21, 984–988.
Loo, A.H., Bonanni, A., Ambrosi, A., Poh, H.L., Pumera, M., 2012. Nanoscale 4, 921–925.
Ludwig, R., Harreither, W., Tasca, F., Gorton, L., 2010. ChemPhysChem 11, 2674–2697.
Ludwig, R., Ortiz, R., Schulz, C., Harreither, W., Sygmund, C., Gorton, L., 2013. Anal. Bioanal. Chem. 405, 3637–3658.
Makarov, V.V., Love, A.J., Sinitsyna, O.V., Makarova, S.S., Yaminsky, I.V., Taliansky, M.E., Kalinina, N.O., 2014. Acta Nat. 6, 35–44.
Matei, D.G., Mukik, H., Golzhauser, A., Turchanin, A., 2012. Langmuir 28, 13905–13911.
Matsumura, H., Ortiz, R., Ludwig, R., Igarashi, K., Samejima, M., Gorton, L., 2012. Langmuir 28, 10925–10933.
Mat Zain, N., Stapley, A.G.F., Shama, G., 2014. Carbohydr. Polym. 112, 195–202.
Mazzei, F., Favero, G., Bollella, P., Tortolini, C., Mannina, L., Antiochia, R., 2015. Int. J. Environ. Health Res. 7, 267–291.
Minteer, S.D., Atanassov, H.R., Luckarift, G.R., Johnson, G.R., 2012. Mater. Today 15, 166–173.
Nadagouda, M.N., Varma, R.S., 2008. Green. Chem. 10, 859–862.
Nune, S.K., Chanda, N., Shukla, R., Katti, K., Kulkarni, R.R., Thilakavathy, S., Mekapothula, S., Kannan, R., Katti, K.V., 2009. J. Mater. Chem. 19, 2912–2920.
Pingarron, J., Yanez-Sedeno, P., Gonzalez-Cortes, A., 2008. Electrochim. Acta 53, 5848–5866.
Philip, D., 2010. Physica E: Low.-Dim. Syst. Nanostr 42, 1417–1424.
Pumera, M., 2011. Mater. Today 14, 308–315.
Pumera, M., Sanchez, S., Ichinose, I., Tang, J., 2007. Sens. Actuat. B 123, 1195–1205.
Raveendran, P., Fu, J., Wallen, S.L., 2003. J. Am. Chem. Soc. 125, 13940–13941.
Saha, K., Agasti, S.S., Kim, C., Li, X., Rotello, V.M., 2012. Chem. Rev. 112, 2739–2779.
Schulz, C., Kittl, R., Ludwig, R., Gorton, L., 2016. ACS Catal. 6, 555–563.
Schulz, C., Ludwig, R., Gorton, L., 2014. Anal. Chem. 86, 4256–4263.
Shah, A.T., Din, M.I., Bashir, S., Qadir, M.A., Rashid, F., 2015. Anal. Lett. 48, 1180–1189.
Singh, D., Rawat, D., Isha, 2016. Bioresour. Bioprocess. 3, 14–21.
Stoica, L., Ludwig, R., Haltich, D., Gorton, L., 2006. Anal. Chem. 78, 393–398.
Tasca, F., Harreither, W., Ludwig, R., Gooding, J.J., Gorton, L., 2011. Anal. Chem. 83, 2042–3049.
Tasca, F., Ludwig, R., Gorton, L., Antiochia, R., 2013. Sens. Actuat. B 177, 64–69.
Taurino, I., Sanzò, G., Antiochia, R., Tortolini, C., Mazzei, F., Favero, G., De Micheli, G., Carrara, S., 2016. Trends Anal. Chem. 79, 151–159.
Valodkar, M., Modi, S., Pal, A., Thakore, S., 2011. Mat. Res. Bull. 46, 384–389.
Wang, L., Wang, E., 2004. Electrochem. Commun. 6, 49–54.
Wang, W., Chen, Q., Jiang, C., Yang, D., Liu, X., Xu, S., 2007. Colloid Surf. A: Physicochem. Eng. ASP 301, 73–79.
Wang, X.J., Falk, M., Ortiz, R., Matsumura, H., Bobacka, J., Ludwig, R., Bergelin, M., Gorton, L., Shleev, S., 2012. Biosens. Bioelectron. 31, 251–256.
Ward, K., Gara, M., Lawrence, N.S., Hartshome, R.S., Compton, R.G., 2013. J. Electroanal. Chem. 695, 1–9.
Wink, T., van Zuilen, S.J., Bult, A., van Bennekom, W.P., 1997. Analyst 122, 43R–50R.
Xiong, J., Wang, Y., Xue, Q., Wu, X., 2011. Green. Chem. 13, 900–904.
Yañez-Sedeño, P., Pingarron, J.M., 2005. Anal. Bioanal. Chem. 382, 884–886.
Yang, W., Wang, J., Zhao, S., Sun, Y., Sun, C., 2006. Electrochem. Commun. 8, 665–672.
Zafar, M.N., Safina, G., Ludwig, R., Gorton, L., 2012. Anal. Biochem. 425, 36–42.
Zamocky, M., Ludwig, R., Peterbauer, C., Hallberg, B.M., Divne, C., Nicholls, P., Haltrich, D., 2006. Curr. Protein Pept. Sci. 7, 255–280.
Zamocky, M., Schumann, C., Sygmund, C., O'Callaghan, J., Dobson, A.D.W., Ludwig, R., Haltrich, D., Peterbauer, C.K., 2008. Prot. Expres Purif. 59, 258–265.
Zargar, M., Amid, A.A., Bakar, F.A., Shamsudin, M.N., Shameli, K., Jahanshiri, F., Farahani, F., 2011. Molecules 16, 6667–6676.